HHS Public Access

Author manuscript

Chem Res Toxicol. Author manuscript; available in PMC 2020 June 17.

Published in final edited form as:

Chem Res Toxicol. 2019 June 17; 32(6): 1123–1133. doi:10.1021/acs.chemrestox.8b00417.

The sulfur mustard analog mechlorethamine (bis(2-chloroethyl)methylamine) modulates cell cycle progression via the DNA damage response in human lung epithelial A549 cells

Yi-Hua Jan[†], **Diane E. Heck**[‡], **Debra L. Laskin**[‖], and **Jeffrey D. Laskin**[†,*]

[†]Department of Environmental and Occupational Health, Rutgers University School of Public Health, Piscataway, NJ, 08854, United States

[‡]Department of Environmental Health Science, New York Medical College, Valhalla, NY, 10595, United States

[‖]Department of Pharmacology and Toxicology, Rutgers University, Piscataway, NJ 08854, United States.

Abstract

Nitrogen mustard, mechlorethamine (bis(2-chloroethyl)methylamine; HN2), and sulfur mustard are potent vesicants that modify and disrupt cellular macromolecules, including DNA leading to cytotoxicity and tissue injury. In many cell types, HN2 upregulates DNA damage signaling pathways including ataxia telangiectasia mutated (ATM), ataxia telangiectasia mutated- and Rad3-related (ATR), as well as DNA-dependent protein kinase catalytic subunit (DNA-PKcs). In the present studies, we investigated crosstalk between HN2-induced DNA damage response and cell cycle progression using human A549 lung epithelial cells. HN2 (1–20 μM; 24 h) caused a concentration-dependent arrest of cells in the S and G2/M phases of the cell cycle. This was associated with inhibition of DNA synthesis, as measured by incorporation of 5-ethynyl-2'-deoxyuridine (EdU) into S phase cells. Cell cycle arrest was correlated with activation of DNA damage and cell cycle checkpoint signaling. Thus, HN2 treatment resulted in time- and concentration-dependent increases in expression of phosphorylated ATM (Ser1981), Chk2 (Thr68), H2AX (Ser139), and p53 (Ser15). Activation of DNA damage signaling was most pronounced in S phase cells followed by G2/M phase cells. HN2-induced cell cycle arrest was suppressed by the ATM and DNA-PKcs inhibitors, KU55933 and NU7441, respectively, and to a lesser extent by VE821, an ATR inhibitor. This was correlated with abrogation of DNA damage checkpoints signaling. These data indicate that activation of ATM, ATR, and DNA-PKcs signaling pathways by HN2 are important in the mechanism of vesicant-induced cell cycle arrest and cytotoxicity. Drugs that inhibit activation of DNA damage signaling may be effective countermeasures for vesicant-induced tissue injury.

Graphical Abstract

[*]Corresponding Author: Jeffrey D. Laskin; Tel: 848-445-0170; Fax: 732-445-0119; jlaskin@eohsi.rutgers.edu.

The authors declare no competing financial interest.

Supporting Information

Supporting Information is available free of charge on the ACS Publications website. DOI: 10.121/acs.chemrestox.8b00417

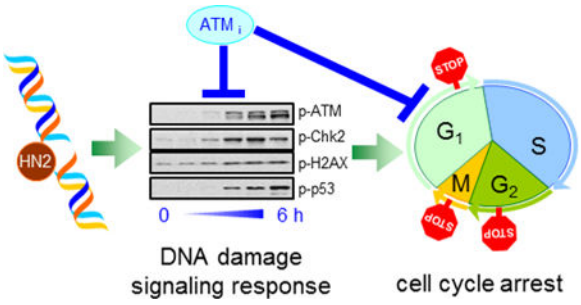

Introduction

Sulfur mustard (2,2′-dichlorodiethyl sulfide, SM) is a potent vesicant that has been used as a chemical warfare agent.[1] The lung is a major target for sulfur mustard, and pulmonary toxicity is a major cause of mortality and long-term complications including bronchitis, bronchiectasis, fibrosis and cancer.[2] Mechlorethamine (bis(2-chloroethyl)methylamine, HN2), a nitrogen mustard and a structural homolog of SM, is used in cancer chemotherapy.[3] Both SM and HN2 are bifunctional alkylating agents that target cellular macromolecules including nucleic acids, proteins, and lipids.[1, 3] Modifications on DNA are the best characterized adducts for mustards which react largely with nucleophilic nitrogen atoms in DNA bases causing the formation of monofunctional adducts on the N7 position of guanine and the N3 position of adenine, and interstrand cross-links such as bis N7-guanine, N7-guanine-N3-adenine and bis N3-adenine adducts.[4–6] Although mustards do not cause DNA strand breaks directly, single and double strand breaks are generated by DNA repair processes.[7, 8] These DNA lesions are capable of blocking DNA replication and transcription, contributing to vesicant-induced cell cycle arrest, mutations and cytotoxicity.[8]

In response to DNA damage, intracellular repair pathways including those mediated by ATM (ataxia telangiectasia mutated), ATR (ataxia telangiectasia and Rad3-related), and DNA-PKcs (DNA-dependent protein kinase catalytic subunit) are activated.[9–11] As serine/threonine protein kinases belonging to the phosphatidylinositol 3-kinase-related kinase (PIKKs) superfamily, these enzymes share similar domain organizations and structural features, however, they have distinct damage specificities and functions.[9] ATM is important in homologous recombination repair of DNA double strand breaks (DSBs) while DNA-PKcs are involved in nonhomologous end joining repair of DSBs.[9, 11] ATR is a replication stress kinase that is recruited to stalled replication forks by a broader spectrum of DNA damage, including DSBs and a variety of DNA lesions that interfere with replication and function in nucleotide excision repair and homologous recombination repair.[10] SM and its analogs are known to activate ATM and ATR by stimulating autophosphorylation on serine 1981 and serine 428, respectively, in multiple human and mouse cell lines.[12, 13] Several ATM/ATR downstream target proteins are also activated in response to mustards including cell cycle checkpoint effectors Chk1, Chk2, the tumor suppressor p53, and the histone variant H2AX.[12–14] Activation of p53, Chk1, and Chk2 checkpoints can slow or arrest cell cycle progression, a process that provides opportunities for cellular and DNA repair, or stimulates cell death if the damage is unrepairable.

In the present studies, mechanisms of HN2-induced DNA damage and repair were investigated using A549 cells, a human lung epithelial cell line. Specifically, crosstalk between DNA damage signaling and cell cycle progression was examined. We found that cytotoxic doses of HN2 caused S phase cell cycle arrest, which was correlated with inhibition of DNA synthesis and activation of DNA damage signaling. Inhibitors of HN2-induced DNA damage sensors on cell cycle progression were characterized. Our findings that antagonists of these sensors limit the inhibitory effects of HN2 on the cell cycle provide support for the idea that the actions of this bifunctional alkylating agent are due, at least in part, to activation of DNA repair. Identification of specific pathways regulating the activity of DNA repair enzymes in lung cells may be useful in the development of efficacious approaches to mitigating morbidity and mortality following exposure to mustards.

Materials and Methods

Caution:

HN2 is a highly toxic vesicant, and precautions were taken for its handling and preparation including the use of double gloves, safety glasses, masks, and other protective equipment to prevent exposures. HN2 waste was disposed of following Rutgers University Environmental Health and Safety guidelines.

Chemicals and Reagents.

Dulbecco's modified Eagle's medium (DMEM; containing 4500 mg/L D-glucose, 110 mg/mL sodium pyruvate, and 584 mg/L L-glutamine; catalog number: 11995–065), fetal bovine serum, penicillin/streptomycin, Click-iT™ EdU Alexa Fluor™ 488 Flow Cytometry Assay Kit, FIX & PERM™ Cell Permeabilization Kit, FxCycle™ PI/RNase Staining Solution, and FxCycle™ Violet were from Life Technologies (Grand Island, NY). SuperSignal West Pico Chemiluminescense Substrate kit was from Thermo Scientific (Rockford, IL) and VE821 was from Sellectchem (Houston, TX). Mechlorethamine hydrochloride, KU55933, protease inhibitor cocktail (catalog no. P2714) which contains 4-(2-aminoethyl)-benzenesulfonyl fluoride, E-64, bestatin, leupeptin, aprotinin, and EDTA, NU7441 and all other chemicals were from Sigma-Aldrich (St. Louis, MO).

Cell Culture and Treatments.

Human A549 lung carcinoma cells were obtained from the American Type Culture Collection (Manassas, VA). Cells were grown in DMEM supplemented with 10% fetal bovine serum, 100 units/mL penicillin, and 100 μg/mL streptomycin in a humidified atmosphere of 5% CO_2 at 37 °C. Components in serum including albumin are known targets for covalent modification by HN2. Thus, solutions of HN2 were freshly prepared before use in serum-free DMEM. For preparation of cellular lysates, A549 cells (5×10^6 cells) were incubated overnight in 15 cm culture dishes and then treated with HN2 (1–500 μM) or vehicle control. After 30 min to 24 h, cells were washed twice with ice-cold PBS (137 mM NaCl, 2.7 mM KCl, 10 mM Na_2HPO_4, 2 mM KH_2PO_4, pH 7.4) and removed from the plates with a cell scraper in 5 mL of PBS. Cell pellets were collected after centrifugation (800 g, 5 min).

For flow cytometric analysis, cells were cultured overnight in 6-well plates (7×10^5 cells/well). Cells were treated with increasing concentrations of HN2 (1–200 μM) or vehicle in serum-free medium. After 30 min to 24 h, cells were harvested using trypsin/EDTA, suspended in 3 mL of 1% BSA in PBS, and cell pellets collected after centrifugation. In some experiments, cells were pre-treated for 30 min with the ATM inhibitor KU55933 (10 μM), the ATR inhibitor VE821 (10 μM), or the DNA-PKcs inhibitor NU7441 (10 μM), followed by concurrent treatment with HN2 (1–20 μM) or vehicle for an additional 24 h.

Preparation of Cellular Lysates and Western Blotting.

Cell pellets were suspended in five volumes of lysis buffer (PBS containing 0.1% Triton X-100 and protease inhibitor cocktail) and sonicated on ice with two 10 s pulses (30 s pulse between two pulses). Cellular debris was removed by centrifugation (800 g, 10 min, 4°C) and the protein concentration of the supernatants quantified with a BCA protein assay kit (Thermo Scientific) with bovine serum albumin as a standard.

For Western blotting, protein samples (50 μg) were subjected to reducing and denaturing SDS-PAGE (4–15% Criterion™ Tris-HCl gel, Bio-Rad, Hercules, CA) followed by electroblotting onto nitrocellulose membranes. Membranes were blocked in 5% nonfat dry milk in PBST (PBS containing 0.1% Tween 20) for 30 min at 37 °C. The blots were reacted with primary antibodies overnight at 4°C, and then with a secondary antibody conjugated to HRP (Bio-Rad) for 30 min at 37 °C. Specific proteins were visualized using chemiluminescence.

Cell Cycle Synchronization.

To synchronize cells in the G1/S boundary, A549 cells (2×10^5 cells/well in 6-well plates) were cultured for 24 h in DMEM without serum followed by 24 h in complete growth medium containing 2 mM thymidine. Cells were then washed once with HBSS and released for synchronized cell cycle progression by refeeding with complete growth medium. After 0–12 h, cell cycle was analyzed in control cells and cells treated with HN2.

Cell Cycle Analysis.

Cells were fixed in 70% ethanol at −20 ºC for 30 min, centrifuged (800 g, 5 min), washed twice with ice-cold PBS, and resuspended in FxCycle™ PI/RNase Staining Solution (1×10^6 cells/mL). Following incubation at room temperature for 30 min, cells were analyzed using a Gallios flow cytometer (Beckman Coulter, Indianapolis, IN); data were analyzed using Kaluza software (Beckman Coulter).

5-Ethynyl-2′-deoxyuridine (EdU) Incorporation Assays.

Incorporation of EdU during DNA synthesis was examined according to the manufacturer's instructions (Life Technologies). Briefly, cells were treated with increasing concentrations of HN2 (1–200 μM) or vehicle in serum-free medium. After 0.5–24 h, cells were incubated with 40 μM EdU in complete medium. After 30 min, cells were harvested and then fixed with 100 μL of Click-iT® fixative solution for 15 min in the dark. Fixed cells were blocked with 100 μL of 1X Click-iT® saponin-based permeabilization and wash reagent for 15 min, followed by incubation with a 1:200 dilution of Alexa Fluor® 488 picolyl azide in PBS

supplemented with 2 mM $CuSO_4$ for 30 min at room temperature. After staining nuclear DNA with FxCycle™ Violet, cell cycle and fluorescently labeled DNA were analyzed by flow cytometry. To examine the cell cycle progression after pulsing with EdU, cells were washed once with HBSS and then cultured with complete growth medium for incremental periods of time from 0 to 12 h before collection and analysis.

Immunocytochemical Detection of DNA Damage Response Proteins.

Following HN2 treatment, A549 cells were dissociated with trypsin-EDTA and washed with PBS containing 1% BSA. Fixation and permeabilization were performed with the FIX & PERM™ Cell Permeabilization Kit according to the manufacturer's directions. Fixed cells were washed with PBS, incubated in 100 μL of blocking buffer (3% BSA in PBS containing 0.5% Triton X-100) for 15 min at room temperature, and then incubated with a 1:50 dilution of Alexa Fluor® 647 conjugated phospho H2AX (Ser139) antibodies (Cell Signaling #9720) or Alexa Fluor® 647 conjugated phospho p53 (Ser15) antibodies (Cell Signaling #8695) in blocking buffer for 1 h at room temperature in the dark. Nuclear DNA was then stained with FxCycle™ Violet and cellular fluorescence analyzed by flow cytometry.

Data Analysis.

All data presented are representative of at least three independent experiments. Statistical analysis was determined using Student's t test and a P value of $p < 0.05$ was considered statistically significant. Graphs were made using the GraphPad Prism 5.0 software (La Jolla, CA) and error bars represented SE ($n = 3–5$).

Results

Mechlorethamine (HN2) induced cell cycle arrest in A549 cells

In initial experiments, we examined the effects of HN2 on cell cycle distribution. In vehicle-treated cells, 73.6% of the cells were in the G0/G1 phase, 15.4% in S phase, and 9.2% in the G2/M phase. Exposure of the cells to HN2 for 24 h caused alterations in cell cycle distribution in a concentration-dependent manner. Whereas at low concentrations (1–2 μM), cells accumulated in G2/M, at higher concentrations (5–20 μM), cells accumulated in S phase. This was associated with a concomitant decrease in cells in G0/G1 (Fig. 1A). Thus, after 2 μM HN2 treatment for 24 h, the percentage of cells in G2/M increased to 30.8% and the percentage of cells in G0/G1 decreased to 28.5%. After 24 h with 10 μM HN2, the percentage of cells in S phase increased to 69.0% and the percentage of cells in G0/G1 was reduced to 16.3% (Fig. 1B). The reversibility of HN2-induced cell cycle arrest was next analyzed in cells treated with HN2 for 24 h followed by recovery in full growth medium for 16–30 h. We found that cell cycle arrest induced by HN2 was partially reversible when cells treated with lower concentrations of HN2 (1–5 μM) in a time- and concentration-dependent manner (Figs. 1A and 1C). Conversely, cell cycle arrest induced by higher concentrations of HN2 (10–20 μM) was irreversible. For cells treated with 1 or 2 μM HN2, an increase of cells in the G0/G1 phases (20–30%) was associated with a decrease of cells in the G2/M phases, measured 16 h after HN2 removal. However, for cells treated with 10 or 20 μM HN2 followed by 16 h recovery in HN2 free medium, a decrease of cells in G0/G1 (10–15%) was associated with an increase of cells in S phase, indicating that the S phase cell cycle arrest

was not reversible. The effects of HN2 on cell cycle arrest were further examined in serum deprivation/thymidine excess synchronized cells. Synchronized cells (t = 0) resulted in 85% of cells in the G1/S border of the cells cycle. After release from thymidine block, cells were in mid S phase at 3 h and entered G2/M by 8 h (Fig S1A). HN2 treatment in the synchronized cells in different cell phases all resulted in G2/M cell cycle arrest by lower concentrations of HN2 and S phase cell cycle arrest by higher concentrations of HN2; these data were similar to findings in asynchronous A549 cells (Figs 1 and S1B).

Expression of cell cycle progression regulatory proteins was next analyzed by Western blotting. In cells treated with low-concentrations of HN2 for 24 h, expression of S and M phase cyclins including cyclin A1, cyclin A2, and cyclin B1 was significantly up-regulated. Additionally, increased phosphorylation of cdc2 on Tyr15 and histone H3 on Ser10, markers for mitosis was noted (Fig. 3). In contrast, higher-concentrations of HN2 down-regulated these proteins, when compared to vehicle-treated controls. HN2 also caused concentration-dependent increases in levels of cyclin E1, a G1/S transition-specific regulator. No differences in the expression of cyclin D1, cyclin D3, total cdc2, or histone H3 were observed between HN2-treated and vehicle-treated controls. These results are consistent with our cell cycle analysis studies showing that low-concentrations of HN2 induced cell cycle arrest in G2/M, while higher-concentrations induced cell cycle arrest in S phase.

In further studies, we examined the effects of HN2 on DNA replication by measuring uptake of 5-ethynyl-2’-deoxyuridine (EdU) into cellular DNA using bivariate flow cytometric analysis. Following vehicle treatment, 21.0% of the cells were in early S phase, 17.3% in mid S, and 2.5% in late S phase (Figs. 4 and 5A). HN2 caused a time- and concentration-dependent reduction in EdU incorporation indicating that HN2 suppressed DNA synthesis (Figs. 2 and 4). Inhibition of DNA synthesis was evident as early as one hour after HN2 treatment. A complete block of DNA replication was detected at 3 h post 200 μM HN2 treatment and 6 h post 50 μM HN2 treatment. The effects of HN2 on cell cycle progression were also examined with EdU in pulse-chase experiments. Cells were treated with HN2 for 30 min and then pulsed with EdU for 30 min; cell cycle progression was then tracked for 12 h post EdU washout. HN2 treatment for 30 min did not affect EdU uptake in A549 cells (Fig 5A, T = 0 h); however, HN2 caused a concentration-dependent delay in the transition of cells through the S phase of the cell cycle. This was observed in cells treated with 1μM HN2. Higher-concentrations of HN2 partially blocked (10 μM) or fully blocked (50 μM) cell cycle progression. Thus, in cells treated with 50 μM HN2, there were no significant changes in the percentage of EdU-positive cells in early, mid and late S phases between EdU washout (T = 0 h) and 12 h post EdU washout. Moreover, in vehicle-treated controls, ten hours after EdU washout, most of the EdU-positive cells completed the cell cycle and returned to G0/G1 phase (24.2% of total cells); however, approximately 12.0% of cells, treated with 1 μM HN2, returned to the G0/G1 phase and 2.5% of cells, treated with 10 μM HN2, returned to the G0/G1 phase. These data are coordinate with our cell cycle analysis showing that high-dose HN2 caused an S-phase cell cycle arrest in A549 cells (Fig. 1A).

HN2 activates DNA damage signaling in a cell cycle phase-dependent manner

DNA damage is known to play a critical role in chemical-induced cell cycle arrest. The effects of HN2 on DNA damage signaling in A549 cells were next assessed. HN2 was found to induce phosphorylation of ATM at Ser1981, a key DNA damage transducer, a response sustained for at least 24 h (Fig. 6). Phosphorylation of downstream ATM targets, including Chk2 at Thr68, H2AX at Ser139 (γH2AX), and p53 at Ser15, also increased in a time- and concentration-dependent manner in response to HN2. Up-regulation of total p53 expression, but not H2AX, was also detected in cells treated with HN2.

Flow cytometry was next used to analyze the effects of HN2 on DNA damage signaling in different phases of the cell cycle. As shown in Figs. 7 and 8, HN2 induced the phosphorylation of H2AX on Ser139 and p53 on Ser15 in a cell cycle phase-dependent manner. A more pronounced induction of these proteins was evident in cells in S phase when compared to cells in G0/G1 and G2/M. These data indicate that cells in S phase are more susceptible to DNA damage induced by HN2. Consistent with our findings from Western blotting experiments, phosphorylation of H2AX and p53 were also time- and concentration-dependent.

Inhibitors of DNA damage kinases abrogate HN2-induced cell cycle arrest

To determine whether inhibition of DNA damage signaling could modulate the inhibitory effects of HN2 on the cell cycle, cells were treated with inhibitors of ATM, ATR, or DNA-PKcs and then analyzed for changes in HN2-induced cell cycle arrest. We found that cells treated with 10 μM of KU55933 (an ATM kinase inhibitor), VE821 (an ATR kinase inhibitor), or NU7441 (a DNA-PKcs kinase inhibitor) were rescued from cell cycle arrest induced by HN2; KU55933 and NU7441 were more effective than VE821 in restoring cell cycle progression (Figs. 9A and 9B). Treatment with KU55933 or NU7441 led to near complete abrogation of cell cycle arrest induced by HN2. These data are consistent with Western blotting, which showed that KU55933 or NU7441 significantly decreased HN2-induced DNA damage signaling including phosphorylation of H2AX and p53 (Fig. 10). In contrast, VE821 treatment only partially decreased DNA damage signaling induced by HN2. Treatment with KU55933, VE821, or NU7441 alone had no effects on DNA damage signaling in A549 cells. Cells treated with KU55933, but not VE821 or NU7441, effectively inhibited the phosphorylation of ATM and Chk2 induced by HN2. These results indicate that DNA damage signaling is a key mechanism of HN2-induced cell cycle arrest.

Discussion

As a bifunctional alkylating agent, HN2 has the capacity to modify and damage cellular DNA.[1, 3] This occurs via the formation of monofunctional DNA adducts as well as intra- and interstrand DNA cross-links.[6, 15] As a result of these modifications, HN2 can modulate cell cycle progression to facilitate DNA repair. The present studies showed that HN2 induced a partially reversible arrest of cells in the G2/M phase at low concentrations (1–2 μM), while at higher concentrations (5–20 μM), arrest of cells in S phase was irreversible. These differential effects of HN2 on cell cycle are in accord with previous studies in rat keratinocytes treated with sulfur mustard.[16] Our findings indicate that DNA damage is

repairable at lower concentrations of HN2, while at higher concentrations, DNA damage is not repairable. This is likely due to differences in the type and extent of DNA modifications at different HN2 concentrations as well as activation of DNA damage response (DDR) pathways. However, it should be noted that HN2 can also form adducts with other cellular components including proteins controlling the cell cycle; it can also form DNA protein cross-links. For example, Jan *et al.*[17, 18] reported that HN2 modifies and cross-links the thioredoxin system, a cellular thio-disulfide reduction system that regulates the activity of proteins important in DNA synthesis and cell cycle control. Using DNA affinity capture techniques, Loeber *et al.*[19] and Michaelson-Richie *et al.*[20] found that HN2 can also form DNA-protein cross-links with enzymes important in regulating cell cycle control, chromatin and transcriptional regulation, as well as DNA replication and repair. Thus, one cannot exclude the possibility that protein-protein and protein-DNA adduct formation at different concentrations of HN2 also differentially affect cell cycle progression.

Mammalian cell cycle transition is controlled by the expression or activities of complexes of cyclin/cyclin dependent kinases (CDKs) and their downstream effectors such as tumor suppressor protein p53 and Rb. These proteins are known to be regulated by a variety of growth factors as well as stress and damage signaling pathways, particularly the DNA damage response.[21] Consistent with our cell cycle analysis findings, HN2 caused a biphasic concentration-dependent response on expression of cyclins. Thus, while lower concentrations of HN2 (1–2 μM) increased expression of cyclin A1 and A2, key regulatory proteins involved in the transition through S and G2/M, and cyclin B1, a G2/M specific cyclin involved in the transition through mitosis, higher concentrations of HN2 (5–20 μM) decreased expression of these proteins as well as the mitotic protein marker, phosphorylated H3 (Ser10). In contrast, higher concentrations of HN2 increased levels of cyclin E. The accumulation of cyclin E in the cells after HN2 exposure likely resulted from a decrease in degradation of the protein by the ubiquitin-proteosome system, a process required to control S phase progression. Stabilization of cyclin E is known to be involved in slowing S phase cell cycle progression and cell cycle arrest in response to DNA damage induced by mitomycin C or UV irradiation and overexpression of its upstream regulatory proteins such as the transcription factor DEC1.[22, 23] Reduction in phosphorylation of H3 on Ser10 by higher concentrations of HN2 is consistent with earlier studies showing S phase arrest in cells exposed to N-nitroso compounds, which are also DNA alkylating agents.[24]

These studies also showed that HN2 caused activation of DNA damage signaling pathways including ATM signaling cascades; thus, HN2 induced the phosphorylation of ATM (Ser1981), Chk2 (Thr68), H2AX (Ser139), and p53 (Ser15) in a time- and concentration-dependent manner. HN2 also upregulated total p53, but not total H2AX proteins, suggesting that HN2 regulates p53 and H2AX, two key DNA damage response proteins, via distinct mechanisms. Of interest were our findings that following HN2 treatment, cells in S phase show significantly more phosphorylation of H2AX and p53 than cells in G2/M and G0/G1 phases, implying more DNA lesions in the S phase than in other phases of the cell cycle. This is in accord with earlier studies showing that cells in S phase are more sensitive to agents known to damage DNA including UV irradiation and DNA topoisomerase inhibitors.[25, 26] It is possible that during DNA replication the DNA duplex is more accessible to alkylating agents. Further studies are needed to explore this possibility.

Using synchronized cells, our studies showed that treatment with HN2 in different phases of the cell cycle show similar effects on cell cycle distribution when compared to asynchronous cells. This occurred despite the fact that cells in S phase were more sensitive to the DNA damage response. Our studies examined cell cycle progression and the DNA damage response 24 h after HN2 treatment. It is possible that the DNA damage response induced by HN2 was not sufficient to suppress cell cycle progression over this time period. Further studies are needed to understand the relationship between the control of cell cycle progression following the DNA damage response.

We also found that cell cycle arrest induced by HN2 was associated with inhibition of DNA synthesis. This may occur as a consequence of the formation of HN2/DNA monoadducts and cross-links that interfere with the progression of DNA replication. Besides DNA damage, other factors, including impaired formation of DNA polymerase complexes, interference with the metabolism of deoxyribonucleotide triphosphates (dNTPs), inhibition of enzymes regulating topological DNA stress, and alterations in signaling pathways, may also introduce replication stress leading to inhibition of DNA synthesis. In this regard, previous studies have shown that DNA interstrand cross-links can affect DNA polymerase activity.[27] Indeed, several proteins that participate in DNA replication are molecular targets for mustard vesicants including DNA topoisomerase I and II, ATP-dependent DNA helicase, and DNA replication licensing factor MCM3.[19, 28] Earlier studies also identified the thioredoxin system, an upstream regulator of ribonucleotide reductase, as a molecular target for HN2, a process that can lead to reduced cellular dNTP pools.[17, 18] This in turn can block DNA synthesis.

A question arises as to whether cell cycle arrest is due to DNA modifications or to the induction of DNA damage response proteins. ATM, ATR, and DNA-PKcs are known to act as apical regulators of the activation of cell cycle checkpoints following DNA damage, leading to a slowing of cell cycle progression, which allows DNA damage to be repaired. Our findings that inhibition of the DDR regulators ATM, ATR, and DNA-PKcs by specific inhibitors (KU55933, VE821, and NU7441, respectively) rescued cell cycle arrest induced by HN2 in A549 cells, suggest that blocking these kinases can override cell cycle checkpoints. This is supported by our observation that inhibition of ATM by KU55933 suppressed HN2-induced checkpoint Chk2 phosphorylation. Abrogation of cell cycle arrest by inhibitors of ATM/ATR/DNA-PKcs have been reported with the action of checkpoint inhibitors such as caffeine or UCN01 on cell cycle arrest caused by ionizing radiation or agents such as cisplatin.[29,30, 31] These data also indicate that cell cycle arrest induced by HN2 may result from activation of DNA damage signaling, but not DNA modifications. It should be noted that the DNA damage response is induced at both low and high concentrations of HN2. Thus, it is unlikely that in our recovery experiments, it is only cells without DNA damage that are recovering. Further studies are needed to better characterize the extent of DNA damage in cells recovering from inhibitors and whether this contributes to alterations in cell progression.

In summary, our studies provide a molecular mechanism of HN2-induced irreversible S phase cell arrest via DNA damage signaling mediated by the ATM-Chk2/p53/H2AX pathway. Inhibition of transducing signals induced by ATM/ATR/DNA-PKcs can effectively

abrogate HN2-induced cell cycle arrest. Therefore, compounds that inhibit activation of DNA damage signaling may be effective countermeasures for vesicant-induced tissue injury.

Supplementary Material

Refer to Web version on PubMed Central for supplementary material.

Acknowledgments

Funding Sources

This work was supported by NIH grants AR055073, NS079249, NS108956, ES004738, and ES005022.

Abbreviations

HN2	mechlorethamine
ATM	ataxia telangiectasia mutated
ATR	ataxia telangiectasia and Rad3-related
DNA-PKcs	DNA-dependent protein kinase catalytic subunit
SM	sulfur mustard
DSBs	DNA double strand breaks
EdU	5-ethynyl-2’-deoxyuridine
DDR	DNA damage response

References

(1). Dacre JC, and Goldman M (1996) Toxicology and pharmacology of the chemical warfare agent sulfur mustard. Pharmacol Rev 48, 289–326. [PubMed: 8804107]

(2). Weinberger B, Malaviya R, Sunil VR, Venosa A, Heck DE, Laskin JD, and Laskin DL (2016) Mustard vesicant-induced lung injury: Advances in therapy. Toxicol Appl Pharmacol 305, 1–11. [PubMed: 27212445]

(3). Singh RK, Kumar S, Prasad DN, and Bhardwaj TR (2018) Therapeutic journery of nitrogen mustard as alkylating anticancer agents: Historic to future perspectives. Eur J Med Chem 151, 401–433. [PubMed: 29649739]

(4). Fidder A, Moes GW, Scheffer AG, van der Schans GP, Baan RA, de Jong LP, and Benschop HP (1994) Synthesis, characterization, and quantitation of the major adducts formed between sulfur mustard and DNA of calf thymus and human blood. Chem Res Toxicol 7, 199–204. [PubMed: 8199309]

(5). Yue L, Zhang Y, Chen J, Zhao Z, Liu Q, Wu R, Guo L, He J, Zhao J, Xie J, and Peng S (2015) Distribution of DNA adducts and corresponding tissue damage of Sprague-Dawley rats with percutaneous exposure to sulfur mustard. Chem Res Toxicol 28, 532–540. [PubMed: 25650027]

(6). Balcome S, Park S, Quirk Dorr DR, Hafner L, Phillips L, and Tretyakova N (2004) Adenine-containing DNA-DNA cross-links of antitumor nitrogen mustards. Chem Res Toxicol 17, 950–962. [PubMed: 15257621]

(7). Laskin JD, Black AT, Jan YH, Sinko PJ, Heindel ND, Sunil V, Heck DE, and Laskin DL (2010) Oxidants and antioxidants in sulfur mustard-induced injury. Ann N Y Acad Sci 1203, 92–100. [PubMed: 20716289]

(8). Panahi Y, Fattahi A, Nejabati HR, Abroon S, Latifi Z, Akbarzadeh A, and Ghasemnejad T (2018) DNA repair mechanisms in response to genotoxicity of warfare agent sulfur mustard. Environ Toxicol Pharmacol 58, 230–236. [PubMed: 29428683]

(9). Blackford AN, and Jackson SP (2017) ATM, ATR, and DNA-PK: The Trinity at the Heart of the DNA Damage Response. Mol Cell 66, 801–817. [PubMed: 28622525]

(10). Saldivar JC, Cortez D, and Cimprich KA (2017) The essential kinase ATR: ensuring faithful duplication of a challenging genome. Nat Rev Mol Cell Biol 18, 622–636. [PubMed: 28811666]

(11). Jette N, and Lees-Miller SP (2015) The DNA-dependent protein kinase: A multifunctional protein kinase with roles in DNA double strand break repair and mitosis. Prog Biophys Mol Biol 117, 194–205. [PubMed: 25550082]

(12). Tewari-Singh N, Gu M, Agarwal C, White CW, and Agarwal R (2010) Biological and molecular mechanisms of sulfur mustard analogue-induced toxicity in JB6 and HaCaT cells: possible role of ataxia telangiectasia-mutated/ataxia telangiectasia-Rad3-related cell cycle checkpoint pathway. Chem Res Toxicol 23, 1034–1044. [PubMed: 20469912]

(13). Jowsey PA, Williams FM, and Blain PG (2012) DNA damage responses in cells exposed to sulphur mustard. Toxicol Lett 209, 1–10. [PubMed: 22119920]

(14). Inturi S, Tewari-Singh N, Agarwal C, White CW, and Agarwal R (2014) Activation of DNA damage repair pathways in response to nitrogen mustard-induced DNA damage and toxicity in skin keratinocytes. Mutat Res 763–764, 53–63.

(15). Osborne MR, Wilman DE, and Lawley PD (1995) Alkylation of DNA by the nitrogen mustard bis(2-chloroethyl)methylamine. Chem Res Toxicol 8, 316–320. [PubMed: 7766817]

(16). Lin PP, Bernstein IA, and Vaughan FL (1996) Bis(2-chloroethyl)sulfide (BCES) disturbs the progression of rat keratinocytes through the cell cycle. Toxicol Lett 84, 23–32. [PubMed: 8597174]

(17). Jan YH, Heck DE, Malaviya R, Casillas RP, Laskin DL, and Laskin JD (2014) Cross-linking of thioredoxin reductase by the sulfur mustard analogue mechlorethamine (methylbis(2-chloroethyl)amine) in human lung epithelial cells and rat lung: selective inhibition of disulfide reduction but not redox cycling. Chem Res Toxicol 27, 61–75. [PubMed: 24274902]

(18). Jan YH, Heck DE, Casillas RP, Laskin DL, and Laskin JD (2015) Thioredoxin Cross-Linking by Nitrogen Mustard in Lung Epithelial Cells: Formation of Multimeric Thioredoxin/Thioredoxin Reductase Complexes and Inhibition of Disulfide Reduction. Chem Res Toxicol 28, 2091–2103. [PubMed: 26451472]

(19). Loeber RL, Michaelson-Richie ED, Codreanu SG, Liebler DC, Campbell CR, and Tretyakova NY (2009) Proteomic analysis of DNA-protein cross-linking by antitumor nitrogen mustards. Chem Res Toxicol 22, 1151–1162. [PubMed: 19480393]

(20). Michaelson-Richie ED, Ming X, Codreanu SG, Loeber RL, Liebler DC, Campbell C, and Tretyakova NY (2011) Mechlorethamine-induced DNA-protein cross-linking in human fibrosarcoma (HT1080) cells. J Proteome Res 10, 2785–2796. [PubMed: 21486066]

(21). Lim S, and Kaldis P (2013) Cdks, cyclins and CKIs: roles beyond cell cycle regulation. Development 140, 3079–3093. [PubMed: 23861057]

(22). Lu X, Liu J, and Legerski RJ (2009) Cyclin E is stabilized in response to replication fork barriers leading to prolonged S phase arrest. J Biol Chem 284, 35325–35337. [PubMed: 19812034]

(23). Bi H, Li S, Qu X, Wang M, Bai X, Xu Z, Ao X, Jia Z, Jiang X, Yang Y, and Wu H (2015) DEC1 regulates breast cancer cell proliferation by stabilizing cyclin E protein and delays the progression of cell cycle S phase. Cell Death Dis 6, e1891. [PubMed: 26402517]

(24). Chen K, Zhang S, Ke X, Qi H, Shao J, and Shen J (2016) Biphasic reduction of histone H3 phosphorylation in response to N-nitroso compounds induced DNA damage. Biochim Biophys Acta 1860, 1836–1844. [PubMed: 27233451]

(25). Zhao H, Traganos F, and Darzynkiewicz Z (2010) Kinetics of the UV-induced DNA damage response in relation to cell cycle phase. Correlation with DNA replication. Cytometry A 77, 285–293. [PubMed: 20014310]

(26). Kurose A, Tanaka T, Huang X, Halicka HD, Traganos F, Dai W, and Darzynkiewicz Z (2005) Assessment of ATM phosphorylation on Ser-1981 induced by DNA topoisomerase I and II

inhibitors in relation to Ser-139-histone H2AX phosphorylation, cell cycle phase, and apoptosis. Cytometry A 68, 1–9. [PubMed: 16184611]

(27). Roy U, Mukherjee S, Sharma A, Frank EG, and Scharer OD (2016) The structure and duplex context of DNA interstrand crosslinks affects the activity of DNA polymerase eta. Nucleic Acids Res 44, 7281–7291. [PubMed: 27257072]

(28). Groehler A. t., Villalta PW, Campbell C, and Tretyakova N (2016) Covalent DNA-Protein Cross-Linking by Phosphoramide Mustard and Nornitrogen Mustard in Human Cells. Chem Res Toxicol 29, 190–202. [PubMed: 26692166]

(29). Playle LC, Hicks DJ, Qualtrough D, and Paraskeva C (2002) Abrogation of the radiation-induced G2 checkpoint by the staurosporine derivative UCN-01 is associated with radiosensitisation in a subset of colorectal tumour cell lines. Br J Cancer 87, 352–358. [PubMed: 12177808]

(30). Kohn EA, Ruth ND, Brown MK, Livingstone M, and Eastman A (2002) Abrogation of the S phase DNA damage checkpoint results in S phase progression or premature mitosis depending on the concentration of 7-hydroxystaurosporine and the kinetics of Cdc25C activation. J Biol Chem 277, 26553–26564. [PubMed: 11953432]

(31). Wang G, Bhoopalan V, Wang D, Wang L, and Xu X (2015) The effect of caffeine on cisplatin-induced apoptosis of lung cancer cells. Exp Hematol Oncol 4, 5. [PubMed: 25937999]

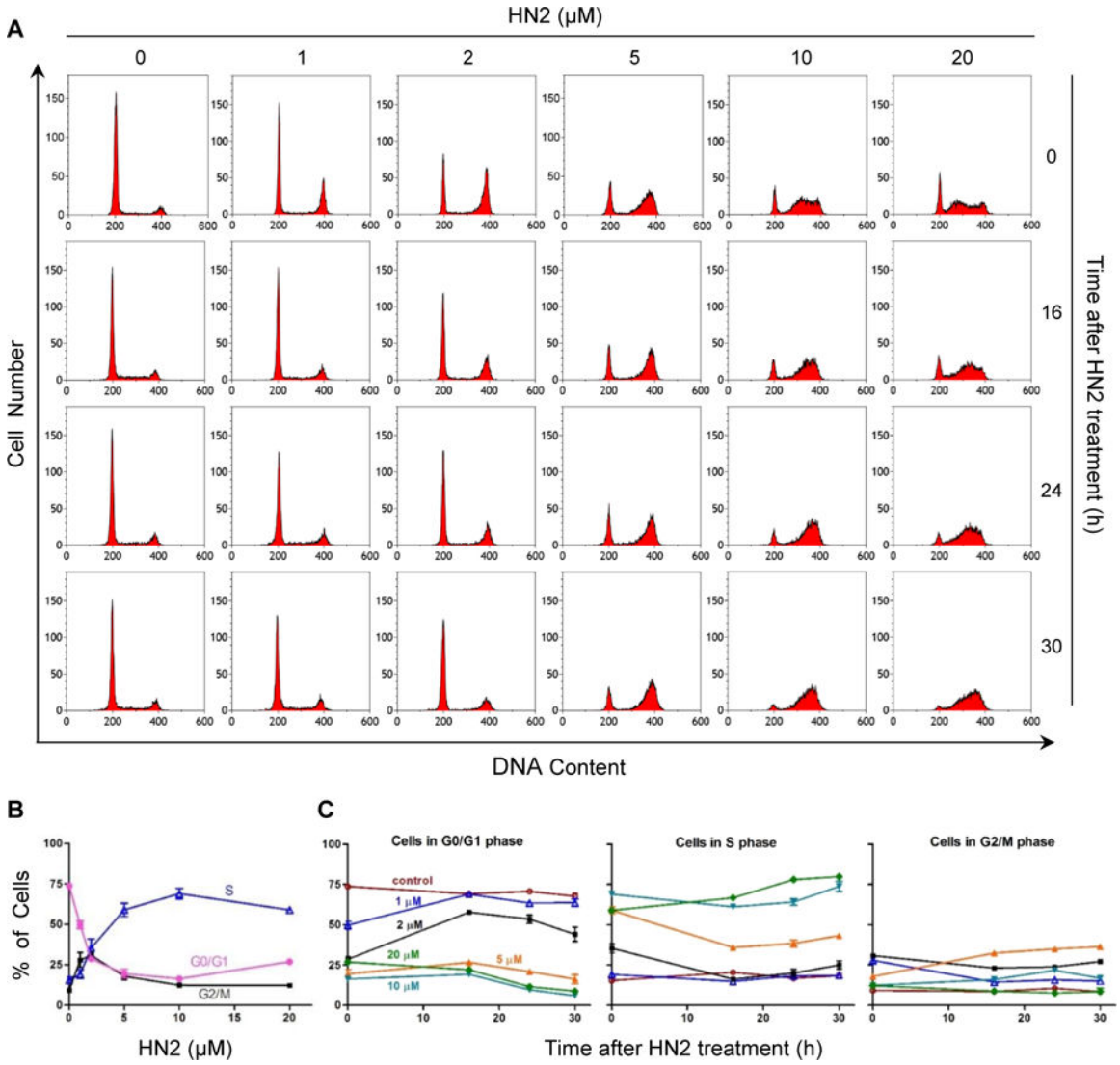

Figure 1. Effects of HN2 on cell cycle distribution in A549 cells.

Cells were treated with increasing concentrations of HN2 (1–20 μM) or vehicle control in serum-free medium. After 24 h, cells were washed and incubated with drug-free complete growth medium for additional 0, 16, 24, and 30 h. Cell cycle distribution was analyzed by flow cytometry using propidium iodide DNA staining. Data are presented as means ± SE, n = 3–5. (A) Representative cytograms showing cell cycle distribution of control and HN2-treated cells. (B) Percentage of cells in each phase of the cell cycle after treatment with HN2 for 24 h. Open triangles, S phase cells; closed circles, G0/G1 phase cells; closed squares, G2/M phase cells. (C) Percentage of cells in each phase of cell cycle after recovery.

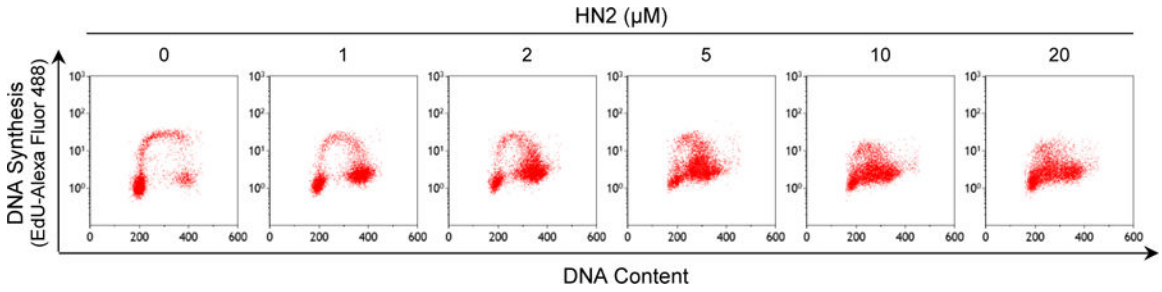

Figure 2. The effects of HN2 on DNA synthesis through the cell cycle in A549 cells.

Cells were treated with HN2 (1–20 μM) or vehicle. After 24 h, cells were washed and incubated with EdU (40 μM) for 30 min. EdU labeled cells were detected using a click reaction with Alexa Fluor® 488 azide. Following DNA staining with FxCycle™ Violet, cells were analyzed by flow cytometry. DNA content is shown on the x-axis (FxCycle™ Violet fluorescence) and DNA synthesis is shown on the y-axis (EdU-Alexa Flour® 488 fluorescence).

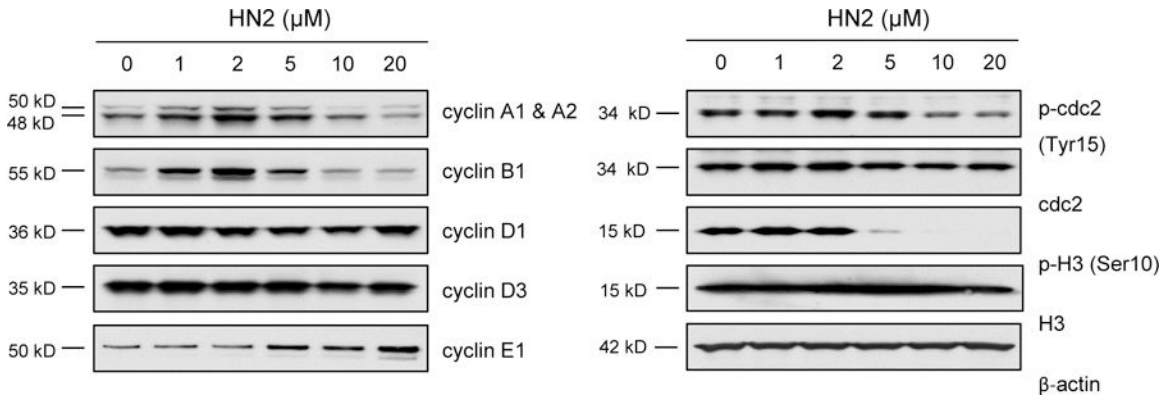

Figure 3. The effects of HN2 on expression of cell cycle regulatory proteins in A549 cells.

Cells were treated with increasing concentrations of HN2 (1–20 μM) or vehicle control. After 24 h, cell lysates were prepared and protein expression analyzed by western blotting. β-Actin was used as an example of a protein loading control. Panel shows representative western blots from one of three independent experiments.

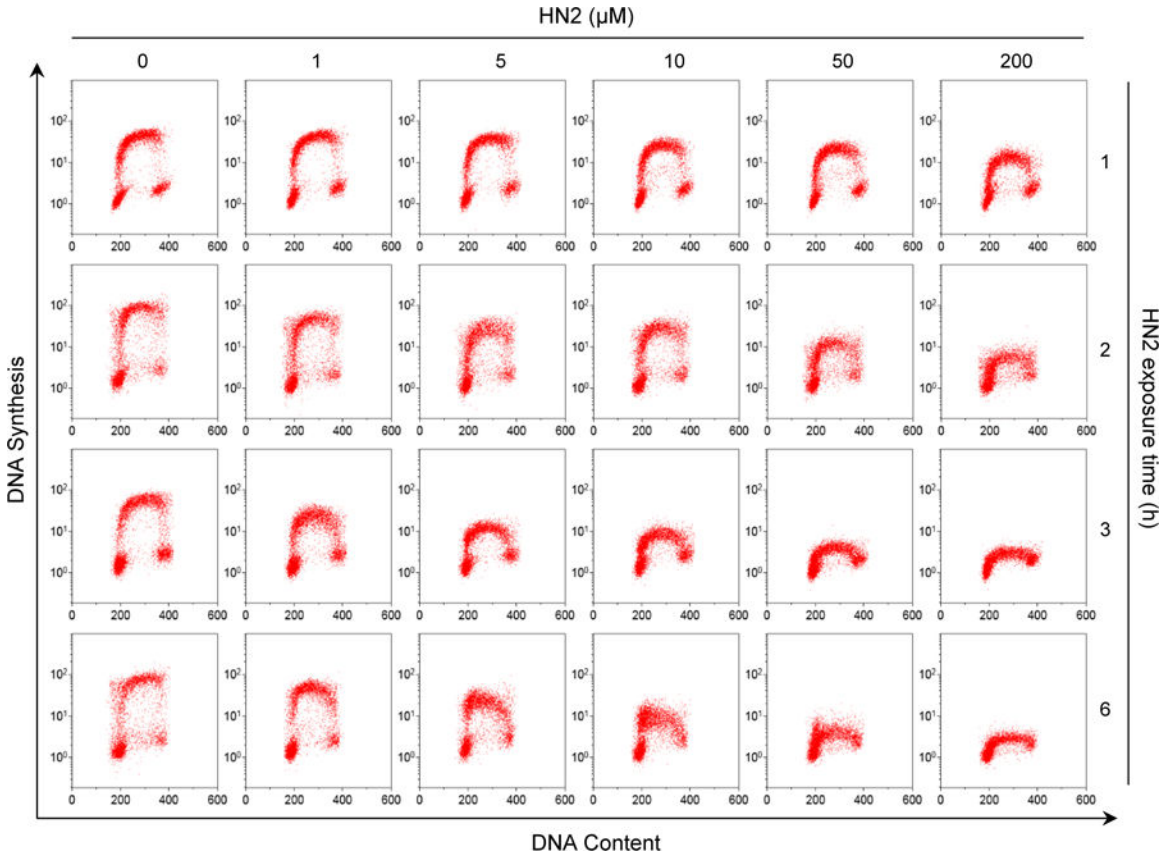

Figure 4. Two color analysis of the effects of HN2 on DNA synthesis in A549 cells.

Cells were incubated with increasing concentrations of HN2 (1–200 μM) or vehicle control in serum-free medium. After the indicated times (1–6 h), cells were pulse-labeled with 5-ethynyl-2'-deoxyuridine (EdU; 40 μM, 30 min). EdU labeled cells were detected using a click reaction with Alexa Fluor® 488 azide. Following DNA staining with FxCycle™ Violet, cells were analyzed by flow cytometry. Representative two parameter histograms are shown from one of three independent experiments. DNA content is shown on the x-axis (FxCycle™ Violet fluorescence) and DNA synthesis is shown on the y-axis (EdU-Alexa Flour® 488 fluorescence).

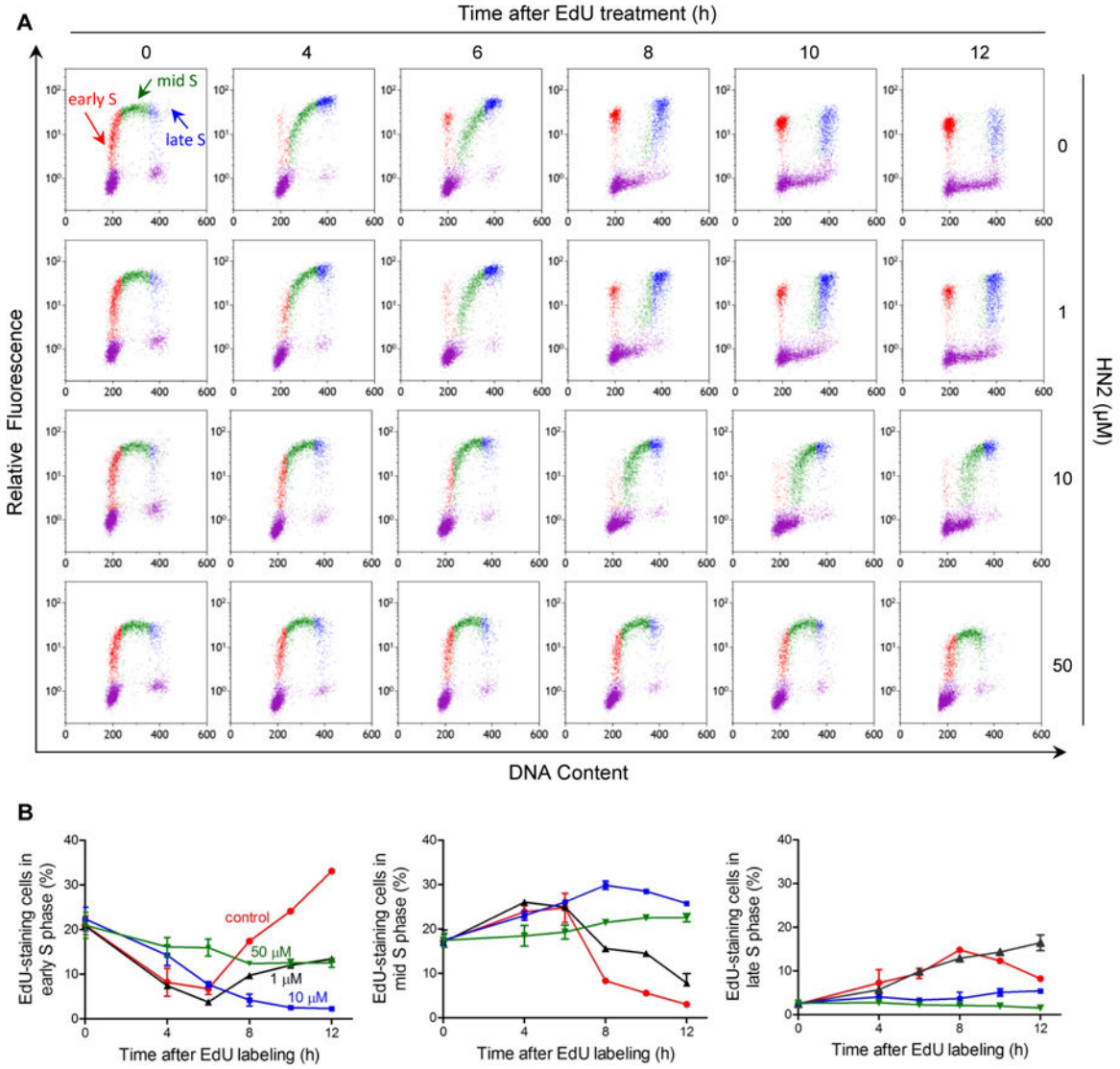

Figure 5. Effects of HN2 on progression of A549 cells through the cell cycle.

(A) EdU pulse-chase assay. Cells were treated with HN2 (10 or 50 μM) or vehicle control in serum-free medium at 37ºC for 30 min followed by 5-ethynyl-2'-deoxyuridine (EdU; 40 μM). After 30 min, cells were refed with complete growth medium without HN2 or EdU. At the indicated times, cells were harvested. EdU labeled cells were detected using a click reaction with Alexa Fluor 488 azide. Following DNA staining with FxCycle™ Violet, cells were analyzed by flow cytometry. Panels show representative two parameter histograms from one of three independent experiments. DNA content is shown on the x-axis (FxCycle™ Violet fluorescence) and DNA synthesis is shown on the y-axis (EdU fluorescence). Cells with no or very low EdU fluorescence, representing cells in G0/G1 and G2/M, are shown in purple. Cells with high EdU fluorescence, representing cells in S-phase, are divided into three groups based on the DNA content: cells with 2N DNA content (early S) are shown in red, cells with 4N DNA content (late S) are shown in blue, and cells with DNA contents in between 2N and 4N (mid S) are shown in green. (B) Percentage of EdU-positive cells in the S phase of the cell cycle.

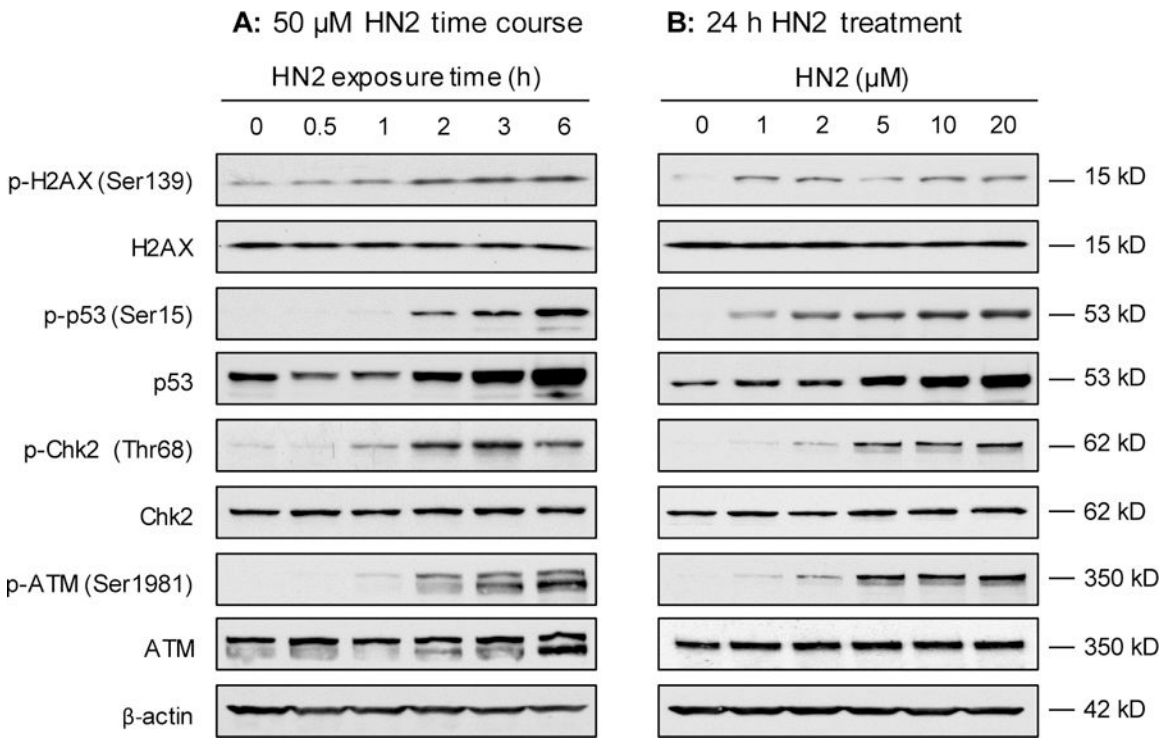

Figure 6. Effects of HN2 on expression of DNA damage response proteins in A549 cells.

Cells were treated with HN2 or vehicle control in serum-free medium. After the indicated times, cells were harvested, lysates prepared, and protein expression analyzed by Western blotting with β-actin as a protein loading control. Representative western blots from three separate experiments are shown. (A) Time-course of changes in DNA damage signaling proteins in response to 50 μM HN2. (B) Effects of increasing concentrations of HN2 on the expression of DNA damage signaling proteins. Protein expression was analyzed 24 h post HN2 treatment.

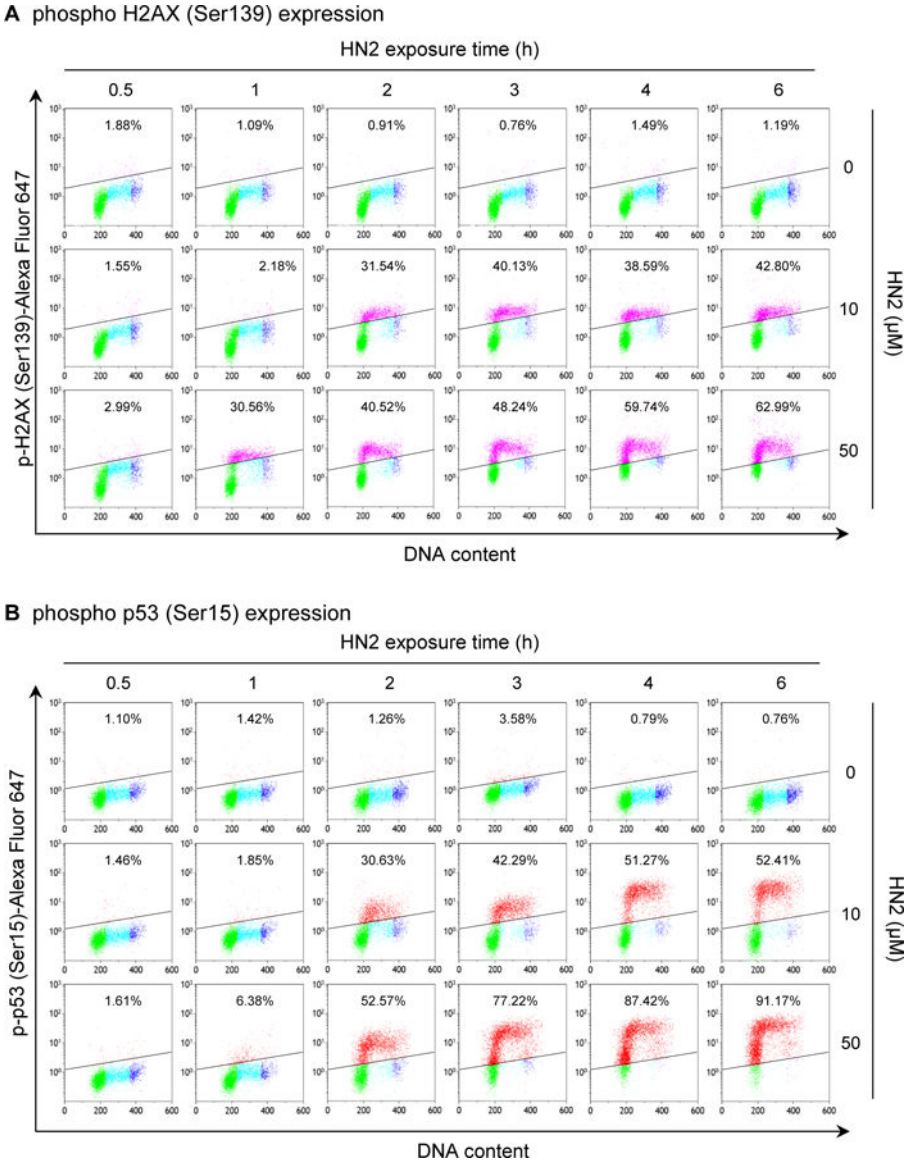

Figure 7. Effects of HN2 on expression of DNA damage response proteins in A549 cells in different phases of the cell cycle.

Cells were treated with increasing concentrations of HN2 or vehicle control in serum-free medium. At the indicated times (0.5–6 h), cells were harvested and stained with fluorescent-conjugated antibodies to phospho H2AX Ser139 or phospho p53 Ser15. DNA was then stained with propidium iodide and the cells analyzed by flow cytometry. Panels show representative bivariate distributions (DNA content vs immunofluorescence) from one of three independent experiments. Panel A, Cells expressing phospho H2AX (Ser139; γH2AX). Phospho H2AX expressing cells are shown in magenta. Panel B, Cells expressing phospho p53 (Ser15). Phospho p53 cells are shown in red. Cell that do not express or express very low levels of phospho H2AX or phospho p53 are shown in green for cells in G0/G1 phase, cyan for cells in S phase, and blue for cells in G2/M phase. The percentage of immunopositive cells is shown at the top of each panel. The line in each panel shows the

upper threshold of phospho-stained immunofluorescence for 95% of interphase cells (G1+S) in vehicle-treated cells.

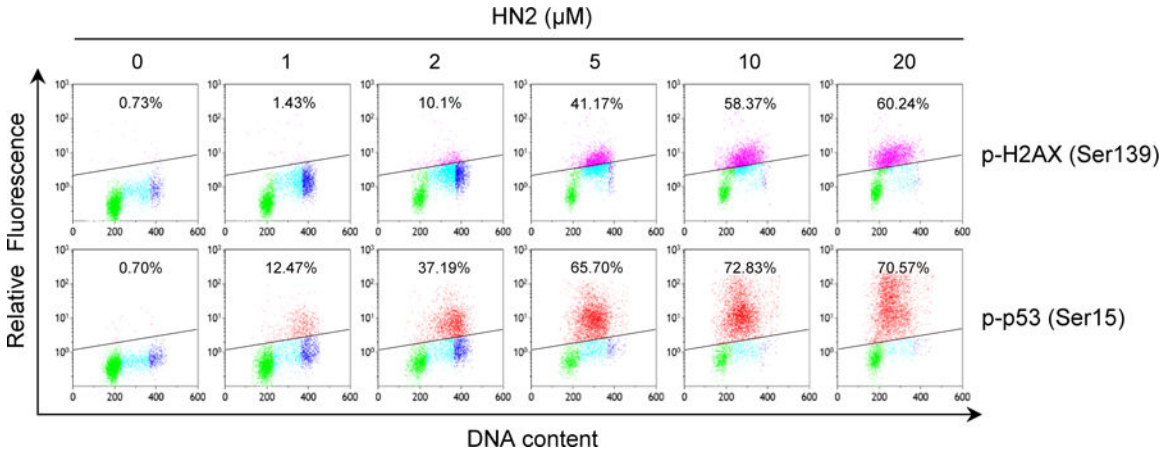

Figure 8. Effects of HN2 on expression of DNA damage response proteins in A549 cells in different phases of the cell cycle.

Cells were treated with increasing concentrations of HN2 or vehicle control in serum-free medium. After 24 h, cells were harvested and stained with fluorescent-conjugated antibodies to phospho H2AX Ser139 or phospho p53 Ser15, followed by propidium iodide; cells were then analyzed by flow cytometry. Panels show representative bivariate distributions (DNA content vs immunofluorescence) from one of three independent experiments. Upper panels, Cells expressing phospho H2AX (Ser139; γH2AX). Phospho H2AX expressing cells are shown in magenta. Lower panels, Cells expressing phospho p53 (Ser15). Phospho p53 cells are shown in red. Cell that do not express or express very low levels of phospho H2AX or phospho p53 are shown in green for cells in G0/G1 phase, cyan for cells in S phase, and blue for cells in G2/M phase. The percentage of immunopositive cells is indicated at the top of each panel. The line in each panel shows the upper threshold of phospho-stained immunofluorescence for 95% of interphase cells (G1+S) in vehicle-treated cells.

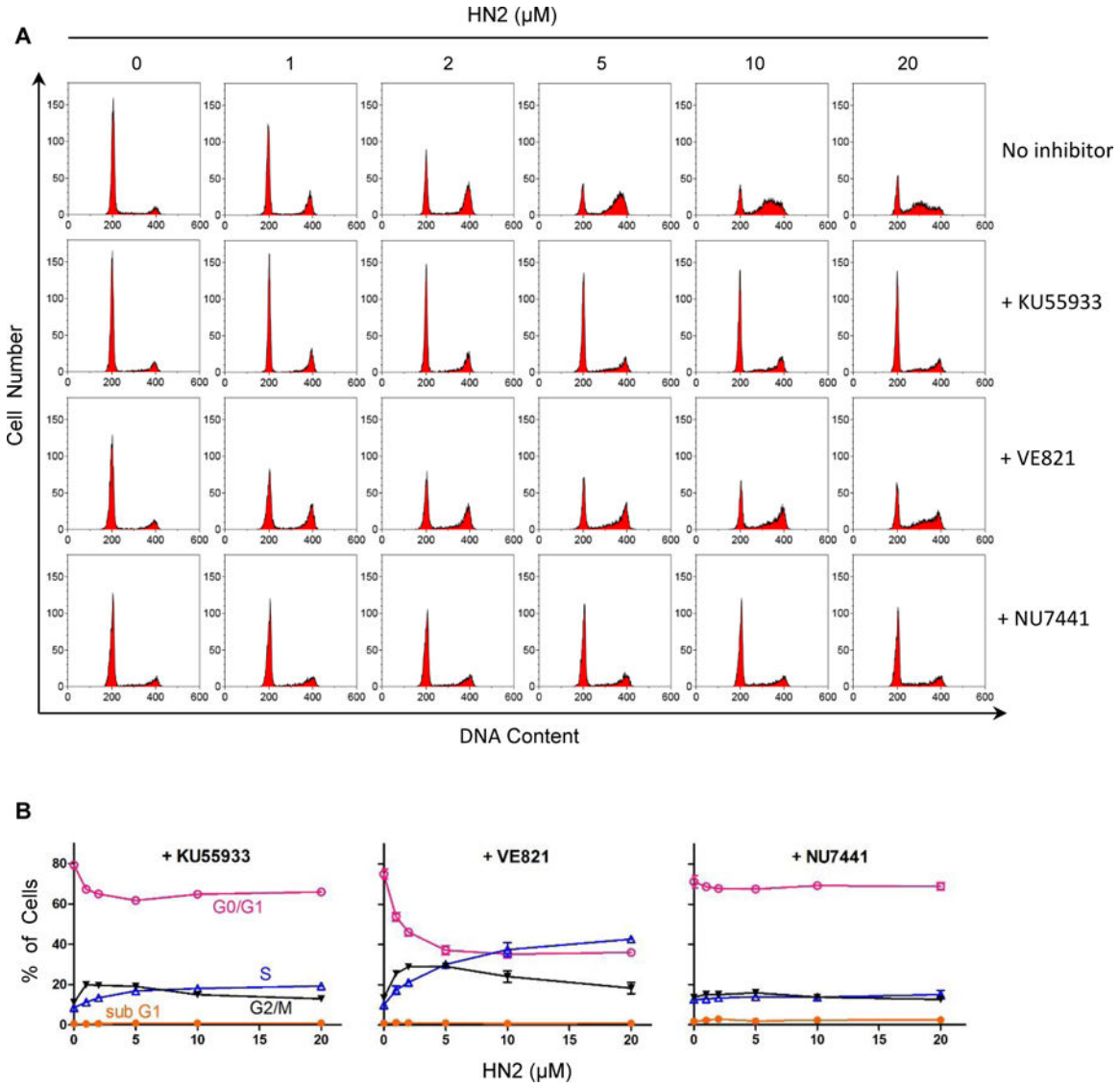

Figure 9. Effects of inhibitors of DNA damage sensing kinase on HN2-induced cell cycle arrest in A549 cells.

Cells were pretreated with 10 μM KU55993 (an ATM inhibitor), VE821 (an ATR inhibitor), NU7441 (a DNA–PKcs inhibitor), or vehicle control. After 30 min, HN2 (1–50 μM) was added to the cultures. Cell cycle analysis was assessed by flow cytometry using propidium iodide DNA staining 24 h after HN2 treatment. (A) Panels show representative cytograms from one of three independent experiments. (B) Percentage of cells in each phase of the cell cycle following treatment with various inhibitors and HN2. Data are means ± SE, n = 3. Open triangles, S phase cells; open circles, G0/G1 phase cells; closed inverted triangles, G2/M phase cells; closed circles, sub G1 phase cells.

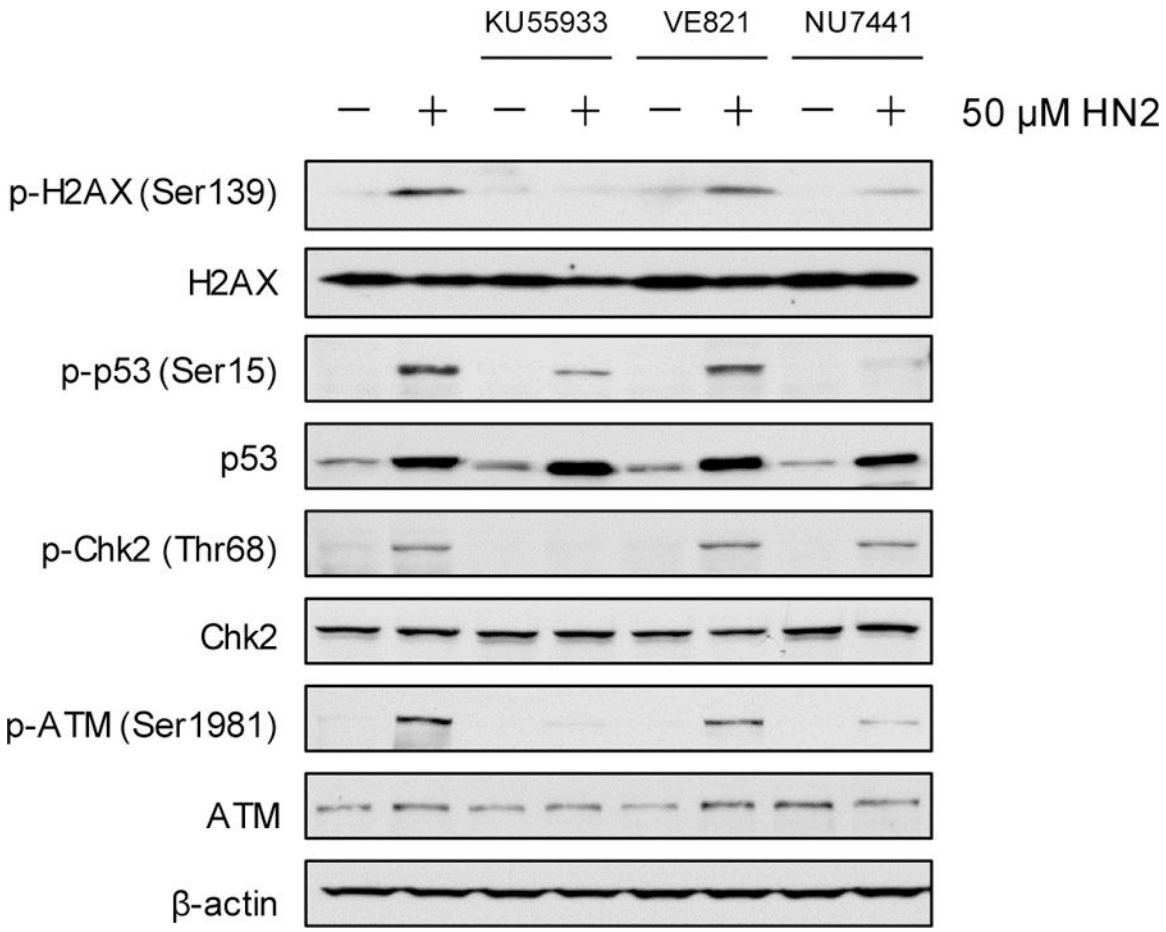

Figure 10. Effects of inhibitors of DNA damage sensing kinase on HN2-induced DNA damage signaling in A549 cells.

Cells were pretreated with 10 μM KU55993 (an ATM inhibitor), VE821 (an ATR inhibitor), NU7441 (a DNA–PKcs inhibitor), or vehicle control. After 30 min, HN2 (50 μM) was added to the cultures. After an additional 3 h, cells were harvested, lysates prepared, and protein expression analyzed by Western blotting with β-actin as a protein loading control.